ARTICLE TYPE www.rsc.org/xxxxxx | XXXXXXXX

To access the final edited and published work see http://dx.doi.org/10.1039/B914478A

Centimetre Scale Assembly of Vertically Aligned and Close Packed Semiconductor Nanorods from Solution

S. Ahmed,[a] Kevin M. Ryan*[a,b]

Received (in XXX, XXX) Xth XXXXXXXXX 200X, Accepted Xth XXXXXXXXX 200X
First published on the web Xth XXXXXXXXX 200X
DOI: 10.1039/b000000x

Assembly of CdS nanorods (8 × 100 nm) into vertically aligned arrays over very large areas on a substrate either as a monolyaer or severaly multilayers is shown by electrophoresis.

Colloidal synthesis of semiconductor nanorods [1-3] and their subsequent organisation [4-11] into vertically aligned and close packed monolayers has attracted significant research interest. In such assemblies, the inherent shape and length dependent properties of discrete nanorods such as linear polarized emission and total photon absorption can be collectively harnessed for scaleable application as light emitting diodes [12] or low-cost nanorod based solar cells.[13, 14] The vertical stacking was initially obtained only by the influence of an electric field on the nanorod dipole during solvent evaporation. [10, 11] Subsequent work with lower aspect ratio rods has shown that vertically aligned and close packed assembly can also occur in the absence of electric fields [4-9] by evaporation control at the solid/liquid or liquid/air interfaces. All studies have shown the importance of several mutually dependent parameters such as rod monodispersity, capping ligand interaction and intermolecular forces on vertical alignment. [15, 16] In addition, such alignment only occurs when the rod concentration in solution is low restricting the assemblies to micrometer sized patches covering less than 5% of the surface. Our investigations of CdS nanorod assembly using both the electric field assisted [11] and the HOPG directed route[4] showed that organisation of close packed perpendicularly aligned monolayers on a substrate is random with individual assemblies containing as few as 10 up to 20,000 nanorods (2 μm^2) (Supporting Information SI1). In effect, the solution is essentially a liquid with dissolved solids and the receding solvent line randomly pins and accumulates rods at successive points on the surface. [17-18] The rate of evaporation and the extent of pinning determines the assembly size. As no accumulation occurs between the pin points the space between the rod assemblies is typically completely absent of particles (SI2).[17-21] The upscaling of vertically aligned nanorod monolayer coverage from random micron sized areas to complete surface coverage is thus restricted in solvent evaporation mediated assembly.

Organisation of nanocrystals at an interface from organic solvents with no evaporation is possible using electrophoresis. Essentially, the influence of an electric field on a charged particle in solution causes electromigration towards and deposition at the oppositely biased electrode. Herman has successfully used this approach to assemble 0D semiconductor nanocrystals into densely packed coatings [22] whereas more recently we have used electrophoresis to selectively assemble gold nanocrystals into lithographic channels with close packed order. [23] In this paper we direct the assembly of 1D nanorods into vertically aligned and close packed assemblies that completely cover centimetre sized substrates. The deposition occurs layer by layer, in a time controlled process, and is independent of rod aspect ratio.

The set-up is shown in Figure 1a where parallel gold coated copper electrodes are completely immersed in a dilute solution of alkylphosphonic capped nanorods in toluene. The ligand capped nanorods are negatively charged and migrate only to the positive electrode under a DC electric field of 200 V forming a conformal deposit. No deposition occurred on the negative electrode [SI3 and SI4]. A substrate consisting of an indium-tin oxide (ITO) square (1 cm × 1 cm) centred on a glass substrate (2 cm × 2 cm) (Fig.1b) was subsequently clamped to the positive electrode and after 5 minutes deposition a smooth conformal yellow deposit was obtained. Coating only occurred only the conducting ITO area with no CdS nanorod deposition on the insulating glass boundary

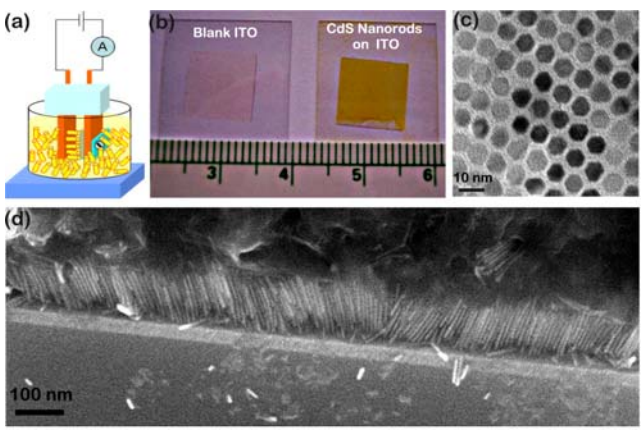

Fig. 1. (a) Schematic of set-up for CdS nanorod assembly by electrophoresis from toluene. The substrate (ITO on glass; silicon wafer; TEM grid) is clamped to the positve electrode under a dc field of 200 V (300-900 s) (b) Photographs of ITO layer on glass (10 mm × 10 mm) before and after CdS rod deposition. (c) TEM image of vertically aligned CdS nanorods deposited on a carbon coated copper grid by electrophoresis. (d) A cross sectional HRSEM image obtained by cleaving the silicon wafer of the aligned nanorod array (8 nm ×

100 nm) on Si/SiO_2 layer (scale bar = 100 nm).

The process was subsequently extended to coating a TEM grid) In transmission mode, the honeycomb framework of close packed rods interspersed with surfactant is clearly visible. Closer inspection reveals the hexagonal faceted shape of the individual wurtzite rods in the superlattice when viewed along the [001] direction. Deposition on a p-type silicon wafer was further succesful. The cross-section of the silicon wafer die (Figure 1d) clearly shows the silicon substrate, SiO_2 (30 nm) and the nanorod deposit (100 nm). Remarkably, the nanorods assemble into an ordered and close packed monolayer coating the entire surface where each nanorod is vertically aligned with respect to the silicon wafer. The capping ligands on the nanorods function both as an organic binder and uniform interparticle spacer (3 nm). Monodispersity in length of the initial rods allows a uniform thickness to be defined in the deposited monolayer. The deposition process is independent of the rod aspect ratio a significant factor in previous approaches influencing preference for perpendicular or parallel assembly This solution phase assembly reproducibly forms perpendicular aligned arrays with only small off axial orientation (~10%) observable in some regions. Tensile stress at the substrate/deposit interface can result in crack propagations after the film is removed from solution and dried [20, 24] however this is significantly reduced when the long chain surfactants are exchanged for pyridine (SI5 and SI6).

The expected mechanism for vertically aligned nanorod deposition is related both to the inherent overall nanorod charge and its constituent dipole moment from its non-centrosymmetric wurtzite lattice. [25] The charge on the CdS nanorod was found to be -51.48 ± 1.44 mV (mobility = -0.12 ± 0.01 $cm^2s^{-1}V^{-1}$) by zeta potential measurements. The overall charge will cause the particle to migrate in solution to the oppositely biased electrode whereas the dipole moment ensures that orientation of the nanorod is parallel to the field lines and hence perpendicular to the substrate on deposition. We ruled out the possibility of dielectrophoresis as a deposition mechanism by altering the electrode configuration to have a non-uniform electric field and sequentially counter biasing the electrodes (SI4). The continued deposition only to the oppositely biased electrode confirmed electrophoresis. Inter-particle repulsion between like charged particles while depositing is expected to be instrumental in the resultant close-packing of the nanorods as it allows particles to find their preferred location in the growing assembly where the potential well of repulsive and attractive forces to neighbouring rods is at a minimum. [23]

Further monolayer HRSEM images from different samples Fig. 2a and SI7 highlight the reproducibility of this technique where in all cases the side to side packing of the nanorods is resolute across the layer allowing the highest possible density of packing to be achieved. Figure 2b shows a HRTEM image of a lift out sample randomly extracted using focussed ion beam milling of a CdS nanorod monolayer deposited on an Au/TaN/Si substrate. The vertical alignment of the rods is evident and occurs regardless of substrate layer. After completion of monolayer coverage subsequent nanorods were found to deposit layer by layer. HRSEM images Fig. 2c-f clearly shows multilayer assembly where two or three highly ordered layers was obtainable by controlling the deposition time. The second depositing layer retains close packing and perpendicular order with the (100 nm × 10 nm) CdS nanorods. Depending on the concentration of excess surfactant in solution, the subsequent layer can deposit directly onto the underlying layer with a negligible gap between the layers as in Fig. 2c or deposit on-top of a 40-60 nm surfactant interlayer as in Fig. 2d. Up to 3 multilayers labeled a, b and c were deposited when the voltage was applied across the solution for 900 s as shown in the cross sectional images (Figure 2e-f).

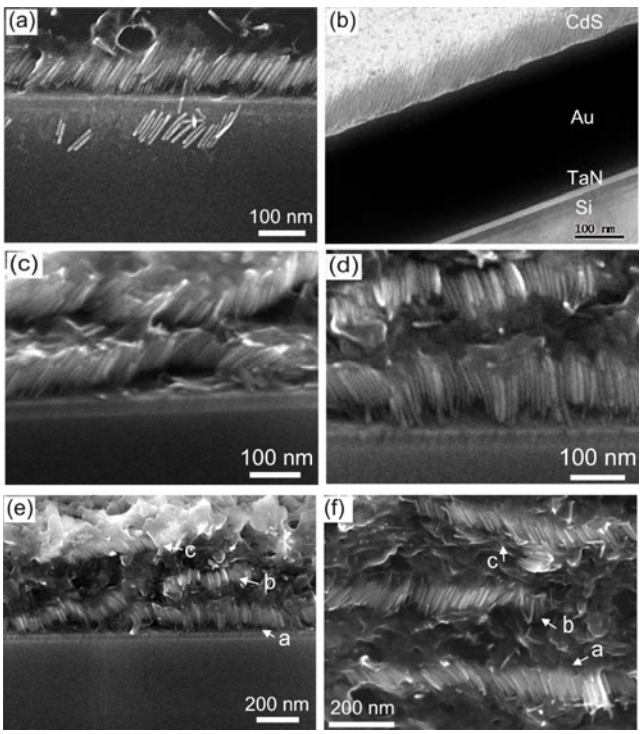

Fig. 2 (a) HRSEM image of CdS nanorod monolayer on Si/SiO_2, after 300 seconds deposition (b) TEM image of FIB lift out sample of CdS monolayer on Au/TaN/Si substrate (300 seconds). (c-d) HRSEM images of bilayers formed after 600 s deposition. (e-f) HRSEM image of multilayer formation on Si/SiO_2 after 900 seconds deposition.

Ohmic indium contacts were placed on perpendicularly aligned nanorod assemblies (2 mm wide × 3 mm long) on Si/SiO_2 to evaluate the electrical characteristics. In the presence of excess ODPA ligands, the vertical nanorod assembly showed little or negligible conductivity due to the insulating inter-rod barrier to electron transport. To remove the ligands, the nanorod solution was subjected to a pyridine reflux prior to electric field mediated deposition. A detailed study of the reflux process showed a propensity for rod elongation through ostwald ripening which had a detrimental affect on the attainment of vertical orientation. An optimised pyridine reflux was determined which resulted in an average inter-nanorod spacing of ~ 1.0 nm and ~75% perpendicular alignment. The I-V curves after ligand removal exhibited leaky Schottky behaviour expected of CdS semiconductor

with a typical conductance of ~130 µS (α in Fig.3a). The increase in conductivity, ~450 µS, (β in Fig.3a) due to the pyridine wash shows that the aliphatic ODPA and TOPO are replaced by aromatic pyridine [26] which is supported by detailed FTIR data (SI8). Replacing a single indium contact with a silver contact created a Schottky junction from which the I-V curve, (Fig.3b) is characteristic of a typical Schottky diode. Repeated capacitance-voltage data was acquired at 150 Hz. The data was analyzed in the framework of the Mott-Schottky model [27] to elucidate the carrier type and density of the CdS nanorods. The data shows n-type CdS with intrinsic doping density, $N_D > 10^{17}$ cm^{-3} (SI9) which is comparable with the literature [28-31] and implies the higher carrier mobility in pyridine washed assemblies.

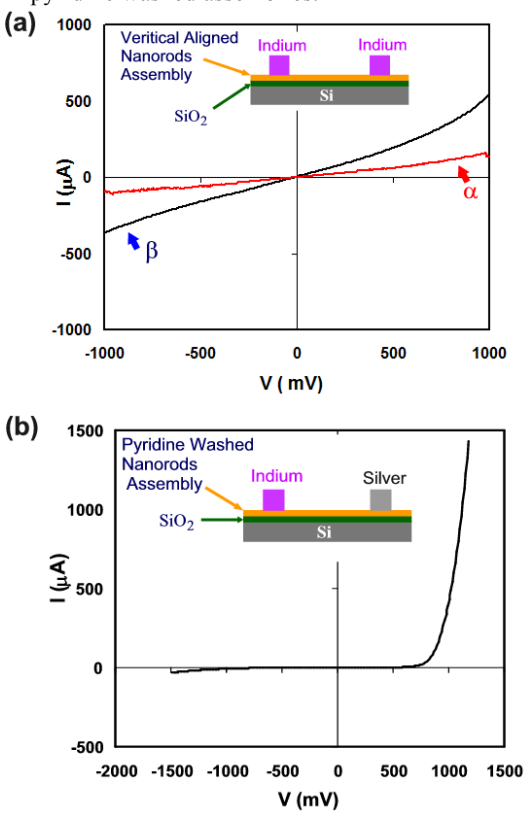

Fig. 3. (a) I-V curves showing leaky Schottky behaviour from the ohmic contact configurations of *indium/ vertical aligned CdS nanorods/indium* (inset schematic). (d) I-V characteristics of a Schottky diode with configurations: silver/*pyridine washed CdS nanorod assembly/indium* (inset schematic) showing typical Schottky diode characteristics.

In conclusion, the results presented here show the capability of controlled electrophoresis as a reproducible method to coat large surface areas with either a single monolayer or multilayers of vertically aligned and close packed nanorods. The scale of organisation (cm^2) is readily amenable to practical application where the unique rod orientation and density of aggregation is desirable. The vertical orientation is independent of rod aspect ratio which is attractive where higher aspect ratios are desired to maximise length dependent properties for example a minimum thickness of ~100-150 nm is required for nanorod based solar cells to ensure total absorption of incident light. [32,33] This method is not limited to II-VI materials and will be generally applicable to any elemental nanorod that can be produced in high yields with monodispersity in length and diameter. In addition to being a low-cost and solution processable route to vertically aligned nanorod layers, the assembly technique is extremely versatile allowing deposition on any substrate that can either be bound to or act as an electrode. Such bulk processable films defined by the position and orientation of each rod at the nanoscale provide a critical link between the demonstrable properties of discrete nanorods or nanorod assemblies and their useable application.

Acknowledgements

The work was supported principally by Science Foundation Ireland (SFI) under the Principal Investigator Program under contract No. 06/IN.1/I85. TEM equipment was facilitated by the Higher Education Authority's Program for Research in Third Level Institutions under INSPIRE. Noel Buckley is further acknowledged for access to Hitachi S4800 HRSEM..

Notes and references

[a] *Materials and Surface Science Institute and Department of Chemical and Environmental Sciences, University of Limerick, Limerick, Ireland;* [b]*SFI-Strategic Research Cluster in Solar Energy Research, University of Limerick, Limerick, Ireland.*

**Corresponding Author to whom correspondence should be addressed E-mail: kevin.m.ryan@ul.ie Tel:+35361213167*

† Electronic Supplementary Information (ESI) available: [Supporting information shows details of any supplementary information available should be included here]. See DOI: 10.1039/b000000x/

1. L. Manna, E. C. Scher, A. P. Alivisatos, *J. Am. Chem. Soc.* 2000, ***122***, 12700.
2. D. J. Milliron, S. M. Hughes, Y. Cui, L. Manna, J. Li, L.-W. Wang, A. P. Alivisatos, *Nature* 2004, ***430***, 190.
3. Z. A. Peng, X. Peng, *J. Am. Chem. Soc.* 2001, ***123***, 183.
4. S. Ahmed, K. M. Ryan, *Nano Lett.* 2007, ***7***, 2480.
5. L. Carbone, C. Nobile, M. DeGiorgi, F. D. Sala, G. Morello, P. Pompa, M. Hytch, E. Snoeck, A. Fiore, I. R. Franchini, M. Nadasan, A. F. Silvestre, L. Chiodo, S. Kudera, R. Cingolani, R. Krahne, L. Manna, *Nano Lett.* 2007, ***7***, 2942.
6. C.-C. Kang, C.-W. Lai, H.-C. Peng, J.-J. Shyue, P.-T. Chou, *ACS Nano* 2008, ***2***, 750.
7. C. O'Sullivan, S. Ahmed, K. M. Ryan, *J. of Mater. Chem.* 2008, ***18***, 5218.
8. D. V. Talapin, E. V. Shevchenko, C. B. Murray, A. Kornowski, S. Förster, H. Weller, *J. Am. Chem. Soc.* 2004, ***126***, 12984.
9. D. V. Talapin, E. V. Shevchenko, C. B. Murray, A. V. Titov, P. Kral, *Nano Lett.* 2007, ***7***, 1213.
10. S. Gupta, Q. Zhang, T. Emrick, T. P. Russell, *Nano Lett.* 2006, ***6***, 2066.
11. K. M. Ryan, A. Mastroianni, K. A. Stancil, H. Liu, A. P. Alivisatos, *Nano Lett.* 2006, ***6***, 1479.
12. J. Hu, L.-S. Li, W. Yang, L. Manna, L.-W. Wang, A. P. Alivisatos, *Science* 2001, ***292***, 2060.
13. I. Gonzalez-Valls, L.-C. Monica, *Energy Environ. Sci.* 2009, ***2***, 19.
14. W. U. Huynh, J. J. Dittmer, A. P. Alivisatos, *Science* 2002, ***295***, 2425.
15. Y. Min, M. Akbulut, K. Kristiansen, Y. Golan, J. Israelachvili, *Nat Mater* 2008, *7*, 527-538.
16. A. V. Titov, P. Kra'l, *Nano Lett.* 2008, ***8***, 3605.
17. R. D. Deegan, O. Bakajin, T. F. Dupont, G. Huber, S. R. Nagel, T. A. Witten, *Nature* 1997, ***389***, 827.
18. T. P. Bigioni, X.-M. Lin, T. T. Nguyen, E. I. Corwin, T. A. Witten, H. M. Jaeger, *Nature Mater.* 2006, ***5***, 265.
19. E. Rabani, D. R. Reichman, P. L. Geissler, L. E. Brus, *Nature* 2003, ***426***, 271.

20. M. P. Pileni, *J. Phys. Chem. B* 2001, ***105***, 3358.
21. J. Tang, G. Ge, L. E. Brus, *The Journal of Physical Chemistry B* 2002, ***106***, 5653.
22. S. Jia, S. Banerjee, I. P. Herman, *The Journal of Physical Chemistry C* 2008, ***112***, 162.
23. S. Ahmed, K. M. Ryan, *Adv. Mater.* 2008, ***20***, 4745.
24. S. Banerjee, S. Jia, D. I. Kim, R. D. Robinson, J. W. Kysar, J. Bevk, I. P. Herman, *Nano Lett.* 2006, ***6***, 175.
25. L.-s. Li, A. P. Alivisatos, *Phys. Rev. Lett.* **2003**, *90*, 974021-974024.
26. J. E. Bowen Katari, V. L. Colvin, A. P. Alivisatos, *The Journal of Physical Chemistry* 1994, ***98***, 4109.
27. S. M. Sze, *Physics of semiconductor devices*, 2nd ed., John Wiley & Sons, New York, 1981, p.286.
28. H. Khallaf, G. Chai, O. Lupan, L. Chow, S. Park, A. Schulte, *Applied Surface Science* 2009, ***255***, 4129.
29. K. Liu, J. Y. Zhang, X. Wu, B. Li, B. Li, Y. Lu, X. Fan, D. Shen, *Physica B: Condensed Matter* 2007, ***389***, 248.
30. E. Bertran, J. L. Morenza, J. E. and, J. M. Codina, *J. Phys. D: Appl. Phys.*, 1984, *17*, 1679-1685.
31. H. L. Kwok, and, K. H. Ho, *J. Phys. D: Appl. Phys.* 1982, ***15***, 2271.
32. Afzaal, P. O'Brien, *J. Mater. Chem.* 2006, ***16***, 1597.
33. K. Ernst, Belaidi, A., and Konenkamp, R. , *Semicond. Sci. Technol.* 2003, ***18***, 475.

: